Microbiome

RESEARCH

Open Access

Modulating the developing gut microbiota with 2′-fucosyllactose and pooled human milk oligosaccharides

Simone Renwick[1], Annalee Furst[1], Mikael Knip[2,3,4], on behalf of the DIABIMMUNE Study Group, Lars Bode[1], Jayne S. Danska[5,6] and Emma Allen-Vercoe[7*]

Abstract

Background Synthetic human milk oligosaccharides (HMOs) are used to supplement infant formula despite limited understanding of their impact on the post-weaned developing gut microbiota. Here, we assess the influence of 0.5 g/L 2-fucosyllactose (2′FL) and 4.0 g/L pooled HMOs (pHMOs) on the composition and activity of cultured fecal-derived microbial communities from seven healthy young children.

Results Exposure to pHMOs induced significant shifts in both the microbial community composition and metabolic output, including an increased abundance of several genera, notably *Bacteroides*, and the production of health-associated metabolites. In contrast, 2′FL alone did not lead to substantial changes in the communities. A total of 330 bacterial isolates, spanning 157 species, were cultured from these communities and individually evaluated for their responses to HMOs. Over 100 non-*Bifidobacterium* species showed enhanced growth upon pHMOs treatment and a high degree of intraspecies variation in HMO metabolism was observed.

Conclusion Our study provides valuable insight into the health-enhancing properties of HMOs while highlighting the need for future research into the efficacy of incorporating individual structures into infant formula, particularly when aiming to modulate the gut microbiota.

Keywords Child gut microbiota, Developing gut microbiota, Human milk, Human milk oligosaccharides, 2′-fucosyllactose, Metabolomics

*Correspondence:
Emma Allen-Vercoe
eav@uoguelph.ca
[1] Family Larsson-Rosenquist Foundation Mother-Milk-Infant Center of Research Excellence (MOMI CORE), the Human Milk Institute (HMI), Department of Pediatrics, School of Medicine, University of California San Diego, La Jolla, CA, USA
[2] Research Programs Unit, Medical Faculty, University of Helsinki, Helsinki, Finland
[3] New Children's Hospital, Helsinki University Hospital, Helsinki, Finland
[4] Tampere Center for Child Health Research, Tampere University Hospital, Tampere, Finland
[5] The Hospital for Sick Children, Toronto, ON, Canada
[6] Department of Immunology and Department of Medicine Biophysics, Faculty of Medicine, University of Toronto, Toronto, ON, Canada
[7] Department of Molecular and Cellular Biology, College of Biological Sciences, University of Guelph, Guelph, ON, Canada

Introduction

Human milk oligosaccharides (HMOs) are a set of structurally diverse, complex carbohydrates that constitute the third largest solid component of human milk. They are composed of more than 150 combinations of five building blocks: glucose, galactose, N-acetylglucosamine, fucose, and sialic acid [1]. Following consumption, HMOs enter the colon undigested, where they perform several functions critical to infant development, such as inhibiting potential pathogens [2], promoting gut barrier function [3], facilitating the development of the immune system [4], and acting as prebiotic substrates for gut microbes [5].

The composition and diversity of HMOs are influenced by polymorphisms in the Secretor (Se) and Lewis (Le) blood group genes, resulting in substantial interpersonal variation among women [6]. Among these, 2'-fucosyllactose (2'FL) is the most abundantly secreted HMO by Se-positive individuals representing ~ 78% of European ancestry populations [7]. Due to its ease of commercial production, 2'FL is the most widely used structure to fortify infant formula [8]. While the studies conducted to date are few, HMO-supplemented formulae have demonstrated some potential health benefits to infants compared to control formulae, such as fewer respiratory tract infections and lower frequencies of eczema, and bronchitis, as well as reduced use of antipyretic and antibiotic drugs [9–12]. Despite these promising findings, our understanding of how HMOs influence the gut microbiota outside the complex matrix of human milk is limited. This knowledge gap is especially relevant given the well-documented protective effects of breastfeeding against childhood diseases associated with the gut microbiota, such as type 1 diabetes (T1D). As such, it is crucial to explore the impact of HMOs when delivered to young children through extended breastfeeding or added to formula. Such investigations could provide insights into the potential of HMOs to modulate the post-weaned developing gut microbiota and inform strategies for enhancing child health.

In this study, we compared the abilities of 2'FL and HMOs pooled from the milk of several women (pHMOs) to modulate the post-weaned developing gut microbiota [13]. Stool donated by seven healthy children, aged 18–24 months, from the DIABIMMUNE cohort [14] was used to seed microbial communities in bioreactors designed to model the human distal colon. pHMOs altered the composition and metabolic output of the microbial communities in contrast to 2'FL alone. A library of 330 bacterial isolates, spanning 157 species, was isolated from bioreactor cultures and evaluated for their ability to metabolize pHMOs in monocultures. We observed both growth-promoting and -inhibiting effects of pHMOs in over 100 non-*Bifidobacterium* species. This research has advanced our knowledge of the microbial growth-supportive properties of HMOs while underscoring the need for further studies on the efficacy of individual structures to modulate the gut microbiota.

Methods

Study participants and sample collection

Stool samples donated by seven young children, aged 18–24 months old, enrolled in the DIABIMMUNE birth cohort [14] were evaluated for this study. Children participating in the DIABIMMUNE study carried human leukocyte antigen (HLA) alleles associated with an increased risk for developing T1D. At the time of stool donation, all seven participants chosen for the present study were free of diabetes or other diseases (Table S1). Children's stool samples were initially collected at home using a custom-made kit and immediately stored at −20 °C in residential freezers. Within one week, the samples were transported to the DIABIMMUNE study center in Helsinki, Finland, where they were stored at −80 °C. Subsequently, the samples were shipped on dry ice to the Hospital for Sick Children, Toronto, ON, Canada, and maintained at −80 °C until use. Samples were cultured at the Allen-Vercoe lab under the University of Guelph REB#17–06-006.

Bioreactor operation and treatment with oligosaccharides

Multifors bioreactor systems (Infors AG, Bottmingen/Basel, Switzerland) were used to model the physiological conditions of the human distal colon as described in Gianetto-Hill et al. [15]. Briefly, vessels were maintained at 37 °C and pH 7 under anaerobic conditions with constant stirring at 50 rpm and a media turnover rate of 24 h. Fecal slurries were prepared under anaerobic conditions (10% H_2, 10% CO_2, balanced with N_2) from 0.5 g stool in sterile, pre-reduced bioreactor media. Each slurry was used to inoculate a 400 mL bioreactor vessel from which samples were collected for subsequent culture. Next, 200 mL vessels containing bioreactor media were inoculated and operated similarly. Vessels were maintained for 14 days to allow the microbial communities to achieve a compositional and metabolic steady-state before the culture was harvested and immediately transferred into an anaerobic chamber. In triplicate, 18 mL of each microbial community was treated with 4.0 g/L pHMOs (previously extracted and purified from milk pooled from several Se-positive individuals (Table S2) [16]), 0.5 g/L 2'FL (Jennewein Biotechnologie GmbH, Rheinbreitbach, Germany), or a no-treatment (water) control, to final volumes of 20 mL. Communities were incubated at 37 °C for 60 h during which samples were collected for cell counting, taxonomic and metabolic profiling, and HMO structure profiling.

Counting cells with flow cytometry

The colony forming units (CFU)/mL of microbial community samples were estimated using a SH800S cell sorter (Sony, San Jose, CA, USA) running in analytical mode to count cells stained with 0.16 μM Syto9 Green Fluorescent Nucleic Acid Stain.

Taxonomic profiling using 16S rRNA gene sequencing

Genomic DNA was isolated using a Zymo Quick-DNA Fecal/Soil Microbe Kit (Cedarlane Laboratories Ltd., Burlington, ON, Canada) with a modified protocol to enhance the lysis of Gram-positive cells. Briefly, 1 mL of

each culture was centrifuged at 14,000 rpm for 15 min. The resulting pellets were resuspended in a lysis buffer in tubes containing 0.2 g of zirconia beads, both supplied by the kit. Samples were homogenized at 3000 rpm for 6 min in a Digital Disruptor Genie3000 (Scientific Industries Inc., Bohemia, NY, USA) before heating to 95 °C for 10 min followed by continuous water bath sonication for 5 min in a Sonicator Ultrasonic Processor XL2020 (Mandel Scientific, Guelph, ON, Canada). Subsequently, samples were treated with 400 µg/mL Recombinant Proteinase K Solution (Ambion, Austin, TX, USA) and heated to 70 °C for 10 min. After cooling, DNA was extracted following the manufacturer's instructions. The concentration and quality of the resulting purified gDNA samples were assessed using a NanoDrop spectrophotometer (Infinite M Nano+, Tecan Group Ltd., Männedorf, Switzerland). 16S rRNA gene library preparation was conducted in-house with 400 ng of Nextera XT Index v2 sequences (Illumina Inc., San Diego, CA, USA) plus standard 16S rRNA gene V4 region primers (515F-GTGYCAGCMGCCGCGGTTA and 806R-GGACTACNVGGGTWTCTAAT) in technical triplicate. The reaction mixture contained 1 µL DNA template (diluted to 10 ng/µL), 1 µL of each barcode/primer, and 23 µL Invitrogen Platinum PCR SuperMix High Fidelity (Life Technologies, Carlsbad, CA, USA). Polymerase chain reaction (PCR) cycling conditions are described elsewhere [17]. Technical triplicates were pooled and purified using an Invitrogen PureLink PCR Purification Kit (Life Technologies, CA, USA) according to the manufacturer's instructions. Normalization of amplicon concentrations and sequencing using a MiSeq Sequencer (Illumina Inc., San Diego, CA, USA) to produce paired-end 300 bp reads were carried out by Advanced Analysis Centre (AAC) Genomics Facility (University of Guelph, ON, Canada).

Sequencing data were processed in R (version 4.2.1) using the DADA2 package [18] (version 1.26) to curate reads into trimmed, quality-controlled, and filtered 200 bp sequences. Sequences were then clustered into amplicon sequence variants (ASVs), which were classified to the genus level by cross-referencing against the SILVA database (version 138). The read counts of ASVs resulting in redundant genera were aggregated before any feature with less than an average of 0.001% relative abundance in at least 1% of samples was removed. Absolute abundance was estimated by normalizing read counts for each taxon to the CFU/mL for the respective sample.

Metabonomic profiling using ^{1}H nuclear magnetic resonance

The metabolic output of the communities was assessed using ^{1}H nuclear magnetic resonance (NMR) as previously described [19]. Briefly, cell-free supernatant was obtained from thawed samples by centrifuging at 14,000 rpm for 15 min and filtering through sterile 0.22 µm-pore size filters. The resulting filtrates were diluted with an internal standard, 99.9% D2O with 5 mM 4,4-dimethyl-4-silapentane-1-sulfonic acid (DSS) and 0.2% sodium azide, to a final concentration of 0.5 mM DSS. Samples were transferred to 5 mm glass NMR tubes (535-PP-7, Wilmad, Wineland, NJ, USA) for scanning in a Brüker Avance 600 MHz NMR spectrometer (AAC NMR Centre, University of Guelph, ON, Canada). Spectra were acquired using the first increment of a 1D ^{1}H NOESY pulse sequence with tmix of 100 ms, 4 s acquisition time, 1 s relaxation delay, and a spectral width of 12 ppm. Chenomx NMR Suite 7.0–7.7 (Chenomx Inc., Edmonton, AB, Canada) was used to process spectra and identify metabolites using the software's 600 MHz compound library. Metabolites were quantified from the area of the projected signal by using the known concentration of DSS and the area of the DSS peak.

Microbial isolation

Microbes were isolated as pure cultures from bioreactor cultures. Briefly, cultures were serially diluted in pre-reduced tryptic soy broth (TSB) supplemented with 5 µg/mL hemin and 1 µg/mL menadione before plating on a variety of selective and non-selective media types (Table S3). Plates were incubated at 37 °C under both aerobic and anaerobic conditions. Over the following 5 days, individual colonies were selected based on varying morphologies and streak purified on fastidious anaerobic agar (FAA) plates. Isolates were identified by first amplifying the V3–V6 region of their 16S rRNA gene using 1 µL of biomass and the primers V3kl (5'-TACGG[AG]AGGCAGCAG-3') and V6r (5'-AC[AG]ACACGAGCTGACGAC-3'). PCR cycling conditions were 95 °C for 15 min (to disrupt the cell membrane), followed by 30 cycles of 94 °C for 2 min, 94 °C for 30 s, 60 °C for 30 s, and 72 °C for 30 s, with a final elongation at 72 °C for 5 min. Nucleotides of the PCR product were fluorescently tagged using a BigDye Terminator v3.1 Cycle Sequencing Kit (Applied Biosystems, ThermoFisher Scientific, Waltham, MA, USA). T7 forward primer (5'-TAATACGACTCACTATAGGG-3') and 25 cycles of 96 °C for 5 min, 96 °C for 30 s, 50 °C for 15 s, and 60 °C for 2 min were used for the fluorescent tagging by the BigDye Terminator. PCR products underwent Sanger sequencing performed by the AAC Genomics Facility. Isolates were identified by cross-referencing their corresponding 16S rRNA gene sequence against the NCBI reference database (https://blast.ncbi.nlm.nih.gov/Blast.cgi). Pure cultures of unique isolates were cryopreserved.

HMO utilization assays

Bacterial isolates were cultured overnight in modified peptone-yeast-glucose (mPYG) broth (Table S4) under anaerobic conditions. mPYG broth diluted 50–75% with water and supplemented with and without 15 g/L pHMOs was inoculated with 5% (v/v) seed culture in biological triplicate in 96-well plates and overlaid with 50 µL mineral oil to prevent evaporation. Plates were incubated at 37 °C for 48 h while optical density (OD600) readings were recorded every 30 min on an Epoch2 microplate spectrophotometer (BioTek Instruments Inc., Winooski, VT, USA) under anaerobic conditions. Samples of spent media were collected at T0 and T48 for each isolate for HMO profiling.

Profiling HMO structures

HMO profiling was performed as previously described [20]. Briefly, a non-HMO oligosaccharide, maltose, was added to each sample to serve as an internal standard. Samples were lyophilized using a speed vacuum prior to labelling with fluorescent 2-aminobenzamide for 2 h at 65 °C. Glycan composition and abundance were analyzed by high-performance liquid chromatography (HPLC). Nineteen HMO structures were identified based on standard retention times: 2'-fucosyllactose (2'FL), 3-fucosyllactose (3FL), 3'-sialyllactose (3'SL), 6'-sialyllactose (6'SL), difucosyllactose (DFLac), difucosyllacto-N-hexaose (DFLNH), difucosyllacto-N-tetrose (DFLNT), disialyllacto-N-hexaose (DSLNH), disialyllacto-N-tetraose (DSLNT), fucodisialyllacto-N-hexaose (FDSLNH), fucosyllacto-N-hexaose (FLNH), lacto-N-fucopentaose (LNFP)1, 2, and 3, lacto-N-hexaose (LNH), lacto-N-tetrose (LNT), lacto-N-neo-tetrose (LNnT), and sialyllacto-N-tetraose (LST) b and c. Total HMO concentration (SUM) was calculated by summing the concentration of each structure. HMO-bound fucose (Fuc) was estimated on a molar basis where each fucose residue on an HMO was counted as one mole. HMO-bound sialic acid (Sia) was calculated accordingly.

Statistical analysis

Statistical analysis was conducted using R (version 4.2.1) using code hosted at https://github.com/SimoneRenwick/Microbiome2024 (accessed on 23rd May 2024). Alpha diversity (Chao1 richness and Shannon diversity index) of the bioreactor communities at steady-state was determined using unfiltered read counts. Beta-diversity at the genus level was assessed using weighted UniFrac and visualized using principal coordinates analysis (PCoA) score plots with non-metric multi-dimensional scaling and permutational multivariate analysis of variance (PERMANOVA, ADONIS). To evaluate the impact of the HMO treatments on longitudinal abundance profiles while controlling for the effects of donor identity, the R package Multivariate Association with Linear Models 2 (MaAsLin2) (version 3.18) [21] was applied. Metabolite concentrations at 60 h were auto-scaled before a principal component analysis (PCA) was used to assess the impact of the HMO treatments on the metabolic output of the communities. Metabolite concentrations at 60 h were also displayed on a heatmap with two-way hierarchical clustering. Significantly different metabolites were identified using multiple analyses of variance (ANOVAs) followed by Tukey's honestly significant difference (HSD) post-hoc tests. Optical density readings collected during the HMO utilization assays on the 330 bacterial isolates were blank corrected against the T0 reading for each well before the average of the three highest optical density readings (ODh) and the area under each growth curve (AUC) was calculated. Multiple *t*-tests were used to assess the impact of pHMOs-treatment on the growth properties of the isolates. Significant correlations among the HMO structures degraded by the isolates and their growth properties were assessed by Spearman rank correlation. Lastly, for species with three or more isolates assayed for their HMO utilization abilities, strain-level heterogeneity was evaluated by k-means clustering of either the fold change in AUC and ODh or the HMO degradation profiles of the isolates. Isolates of the same species that consistently clustered together were determined to be homogeneous in their ability to utilize HMOs, while the separate clustering of isolates of the same species indicated cases of heterogeneity. All *p*-values were corrected for multiple hypothesis testing using the Benjamini–Hochberg method. *Q*-values below 0.05 were considered significant.

Results

HMOs were quickly degraded by the microbial communities

To compare the impact of pHMOs and 2'FL on the composition and activity of the early childhood gut microbiota, steady-state fecal-derived microbial communities [15, 17] were subjected to 4.0 g/L pHMOs, 0.5 g/L 2'FL, or a no-treatment control in triplicate under anaerobic, batch fermentation conditions. Over the following 36 h, the degradation of 19 common HMO structures, as well as HMO-bound fucose (Fuc) and HMO-bound sialic acid (Sia), were monitored (Fig. 1A, B). Overall, 91.0 ± 5.4% of the quantified structures in the pHMOs mixture were degraded within 24 h of treatment. In particular, 2'FL was the most efficiently metabolized structure with the majority degraded within 3 h, whether when administered as part of the pHMOs mixture or in isolation. The incomplete degradation of 3FL, 6'SL, DFLac, and LNFP3 may be the result of an overlap between added HMO structures and

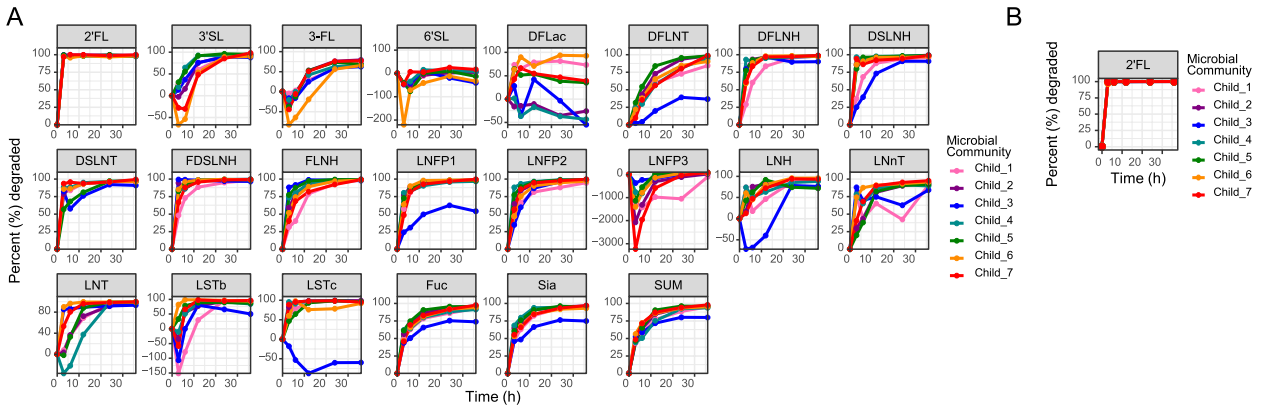

Fig. 1 HMOs were quickly degraded by the microbial communities. **A** Percent (%) of HMO structures degraded by the microbial communities following treatment with 4.0 g/L pHMOs. **B** Percent (%) of 2'FL degraded by the microbial communities following treatment with 0.5 g/L 2'FL alone

HMOs produced from the degradation of larger structures. Repeatedly, fecal-derived microbiota from Child_3 deviated from the other six communities by displaying a lesser ability to degrade DFLNT, LNFP1, and LNH, while increasing the concentration of LSTc.

pHMOs altered microbial community composition

Taxonomic composition of the microbial communities was assessed using 16S rRNA gene sequencing (V4 region). Prior to the HMO treatments, these communities varied in their alpha diversity evident in their Chao1 richness and Shannon diversity index (Fig. 2A). We performed ADONIS (PERMANOVA) analyses to evaluate the effects of donor and treatment on community composition using weighted UniFrac distances. The analysis showed that donor identity had a significant influence at each individual time point (Fig. S1) and cumulatively across all samples and time points (pseudo-F = 114.26, $R^2 = 0.69$, $p = 0.001$; Fig. 2B). In contrast, the effect of treatment was detectable only at the 60-h time point (Fig. S1) but was also significant when all time points were analyzed together (pseudo-F = 5.58, $R^2 = 0.03$, $p = 0.001$; Fig. 2C). We then used MaAsLin2 to analyze the cumulative longitudinal data to identify genera significantly impacted by treatment while controlling for donor identity (Fig. 2D, E and Table S5). Among the genera that expanded following treatment, species of *Bacteroides*, *Ruminococcus*, and *Escherichia-Shigella* demonstrated the largest increases in absolute abundance, while the abundances of several taxa, including *Sutterella*, *Parasutterella*, and *Sellimonas*, declined (Fig. 2D, E). In contrast to these effects of pHMOs, 2'FL treatment did not induce genus-level changes in composition.

pHMOs influenced the metabolic output of the microbial communities

Metabolic output of the microbial communities was measured in culture supernatants using NMR. PCA revealed that the pHMOs-treated communities expressed a unique functional profile compared to those treated with 2'FL alone or the no-treatment control (Fig. 3A). Of the 47 quantified metabolites (Fig. S2), 18 were upregulated by pHMOs, including several amino acids and the short-chain fatty acid (SCFA), acetate (Fig. 3B) (Table S6). In addition, pHMOs treatment suppressed the production of select metabolites such as p-cresol. In contrast, the metabolic concentrations resulting from treatment with 2'FL alone largely reflected the control condition. Only the Child_3 community displayed notable shifts in metabolic output following incubation with 2'FL.

Growth of a wide diversity of species impacted by pHMOs

Next, we examined the growth properties of 330 bacterial isolates (Table S7), spanning 157 species, following treatment with 15 g/L pHMOs or a no-treatment control. These incubations were performed in complex media, rather than minimal media, to allow the manifestation of both positive and negative growth effects compared to baseline growth. Bacterial isolates displayed varying growth strategies following pHMOs supplementation, including logistic growth (Fig. 4A), diauxic or oscillatory growth (Fig. 4B), growth following a long lag phase (Fig. 4C), growth attaining a lower carrying capacity compared to the control condition (Fig. 4D), and growth followed by a death phase (Fig. 4E). A complete inhibition of growth in the presence of pHMOs was also observed for several isolates (Fig. 4F). All growth curves can be found in Fig. S3. To evaluate these properties, the AUC and ODh were calculated and compared for each treatment (Table S8). In total, 193 isolates (101 species) produced a larger AUC following treatment compared to controls as determined by multiple *t*-tests (q-value < 0.05). The largest increases in AUC following supplementation with pHMOs were observed for isolates of *Faecalibacterium prausnitzii, Alistipes onderdonkii*, *Tyzzerella nexilis,* and

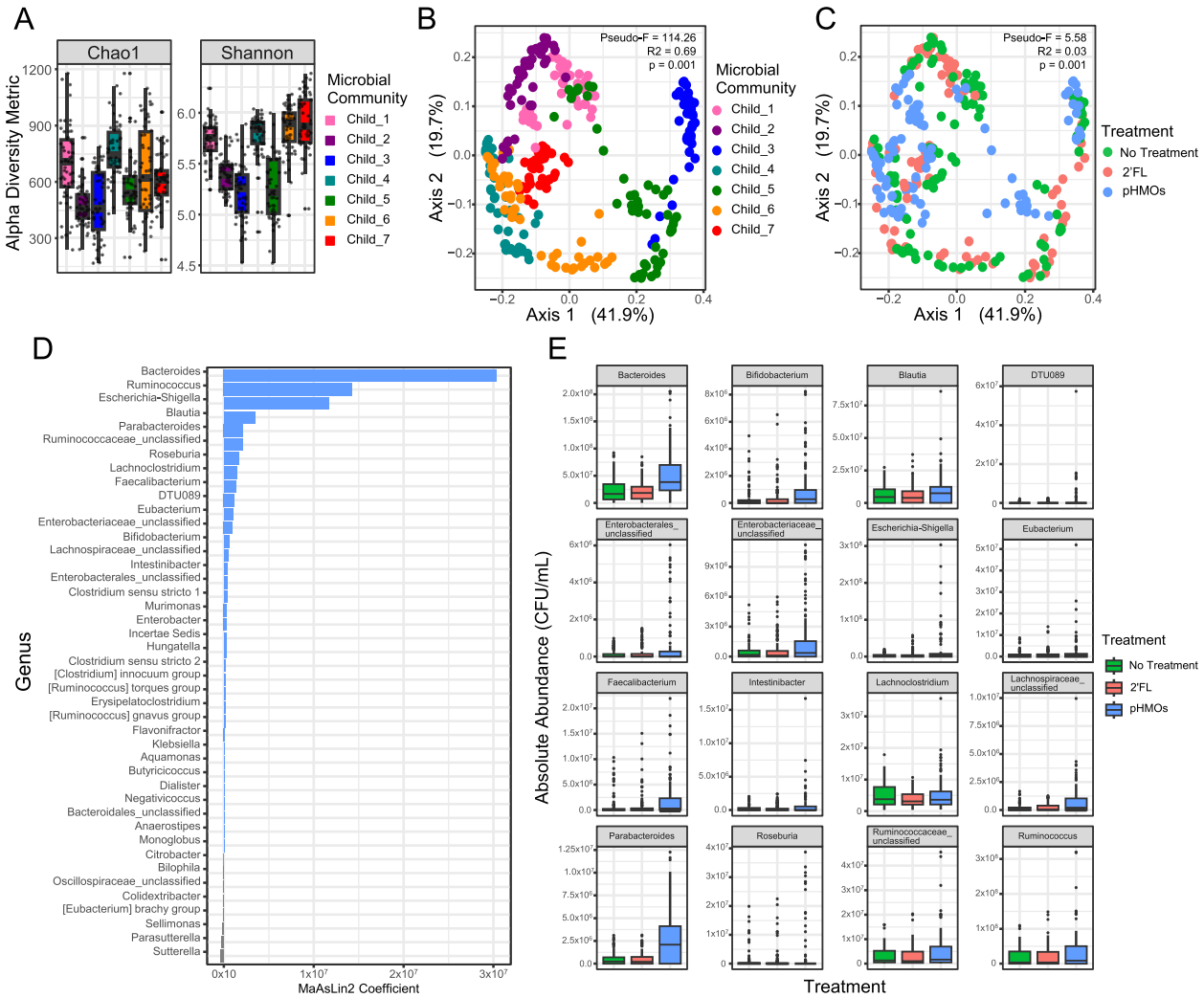

Fig. 2 pHMOs addition altered microbial community composition. **A** Chao1 richness and Shannon diversity index of microbial communities prior to treatment with HMOs. **B**–**C** Weighted UniFrac of all samples collected following treatment of the microbial communities with 4.0 g/L pHMOs, 0.5 g/L 2'FL, or no treatment colored by **B** microbial community or **C** treatment. Significance was determined using ADONIS (PERMANOVA) analyses. **D** MaAsLin2 coefficient of genera significantly affected by pHMOs treatment. **E** Absolute abundance of genera most affected by pHMOs treatment

Bifidobacterium spp. Conversely, 40 isolates (34 species) produced a lower AUC following treatment compared to controls (q-value < 0.05). These included isolates that achieved a lower cell density in the presence of pHMOs as well as those completely inhibited by the oligosaccharides. Furthermore, pHMOs resulted in a higher ODh for 189 isolates (97 species) while 32 isolates (30 species) achieved a lower ODh (q-value < 0.05).

Structure-specific and prolific degradation of HMOs

To assess the HMO structure preferences of the bacterial isolates, spent monoculture media collected at 48 h were profiled for 19 common HMO structures. The structure profiles of the top 100 HMO-degrading isolates are displayed in Fig. 5 while all profiles are found in Fig. S4. Structure specificities varied widely with some isolates able to metabolize numerous structures, such as members of *[Ruminococcus] gnavus*, *Akkermansia muciniphila*, *Bacteroides* spp., and *Bif. bifidum*. Several taxa displayed structure-based specificity including isolates of *Flavonifractor plautii,* which preferentially degraded DSLNT and LNFP3. Overall, sialylated structures were metabolized to a larger extent than fucosylated structures with DSLNT being the most widely utilized HMO, followed by LNFP3, 2'FL, LNnT, and 6'SL. Overall, degradation of fucosylated structures such as 2'FL, LNFP1 and 2, and DFLNT were strongly correlated (Spearman $\rho > 0.6$; $p < 0.001$). Sialylated structures, 3'SL, LSTc, DSLNH, and DSLNT, displayed a similar but weaker co-association (Spearman $\rho > 0.4$; $p < 0.001$) (Fig. S5). The degradation

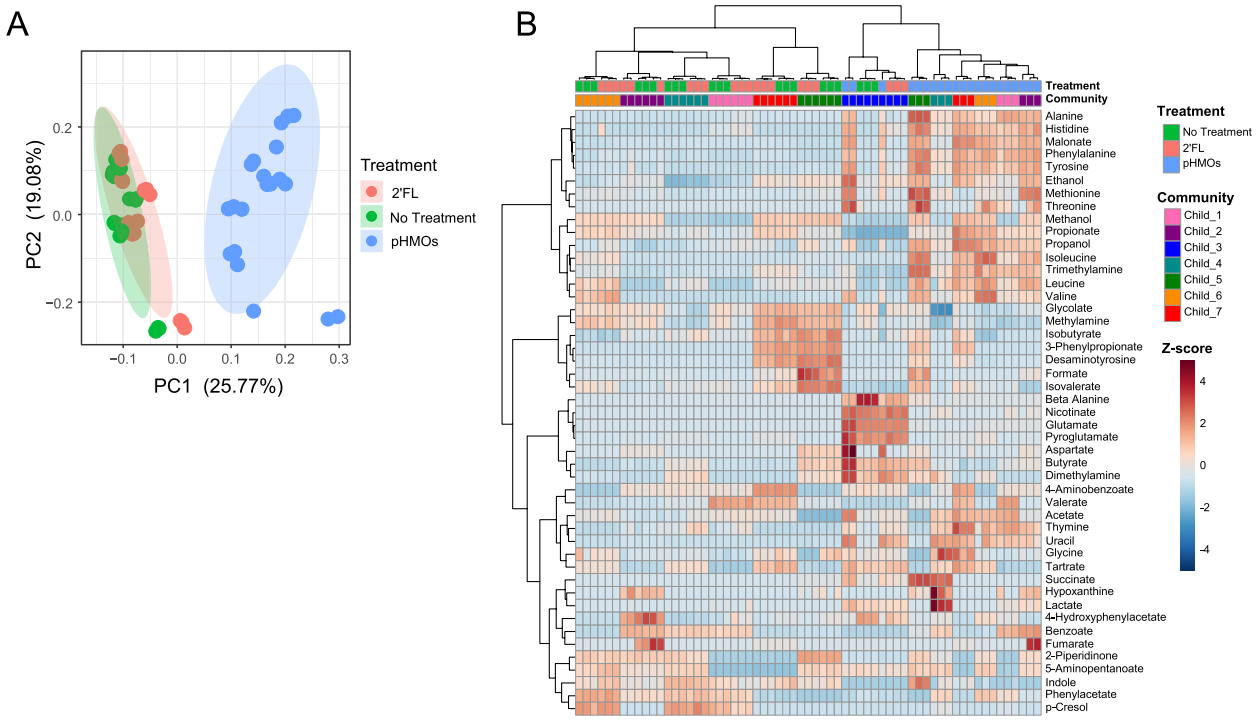

Fig. 3 pHMOs treatment impacted the metabolic output of the microbial communities. **A** Principal component analysis (PCA) of the metabolic output of the microbial communities 60 h following treatment with 4.0 g/L pHMOs, 0.5 g/L 2′FL, or no treatment. **B** *Z*-score normalized concentration of metabolites produced by the microbial communities 60 h following treatment with 4.0 g/L pHMOs, 0.5 g/L 2′FL, or no treatment

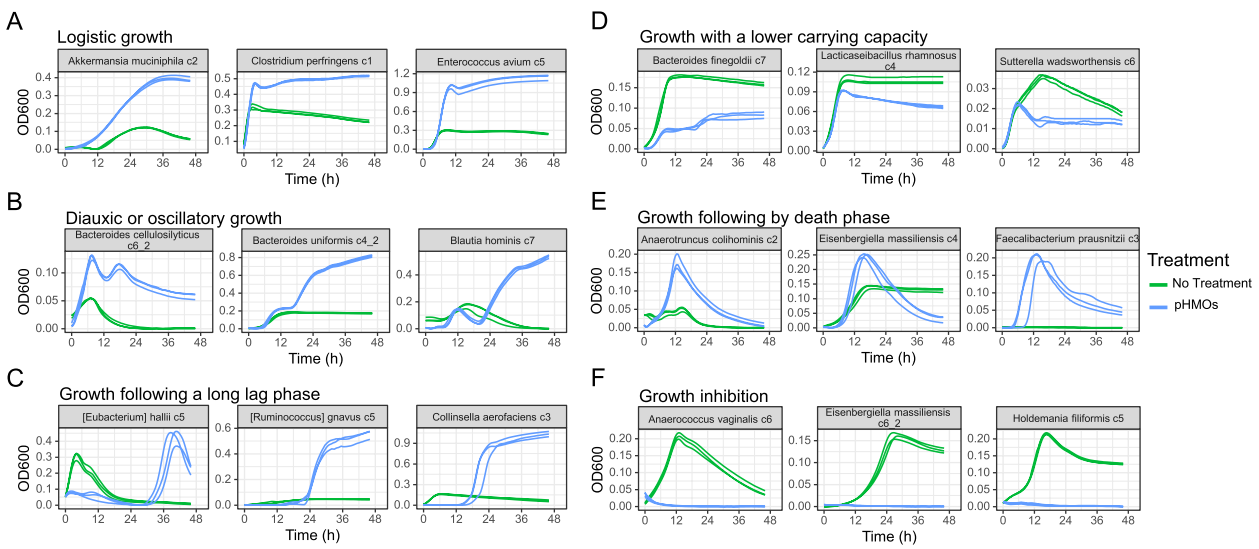

Fig. 4 Growth curves demonstrating diverse growth strategies employed by bacterial isolates in the presence of pHMOs. **A** Logistic growth. **B** Diauxic or oscillatory growth. **C** Growth following a long lag phase. **D** Growth with a lower carrying capacity compared to the control. **E** Growth followed by a death phase. **F** Growth inhibition

of LNT was weakly correlated with AUC ($\rho = 0.37$; $p < 0.001$) as isolates capable of metabolizing LNT exhibited the largest increases in growth relative to controls. No significant correlations were observed between the preferentially degraded structures and other growth curve feature (logistic, logistic-decay, diauxic, long-lag phase, suppressed, or inhibited growth) or with the isolate's donor.

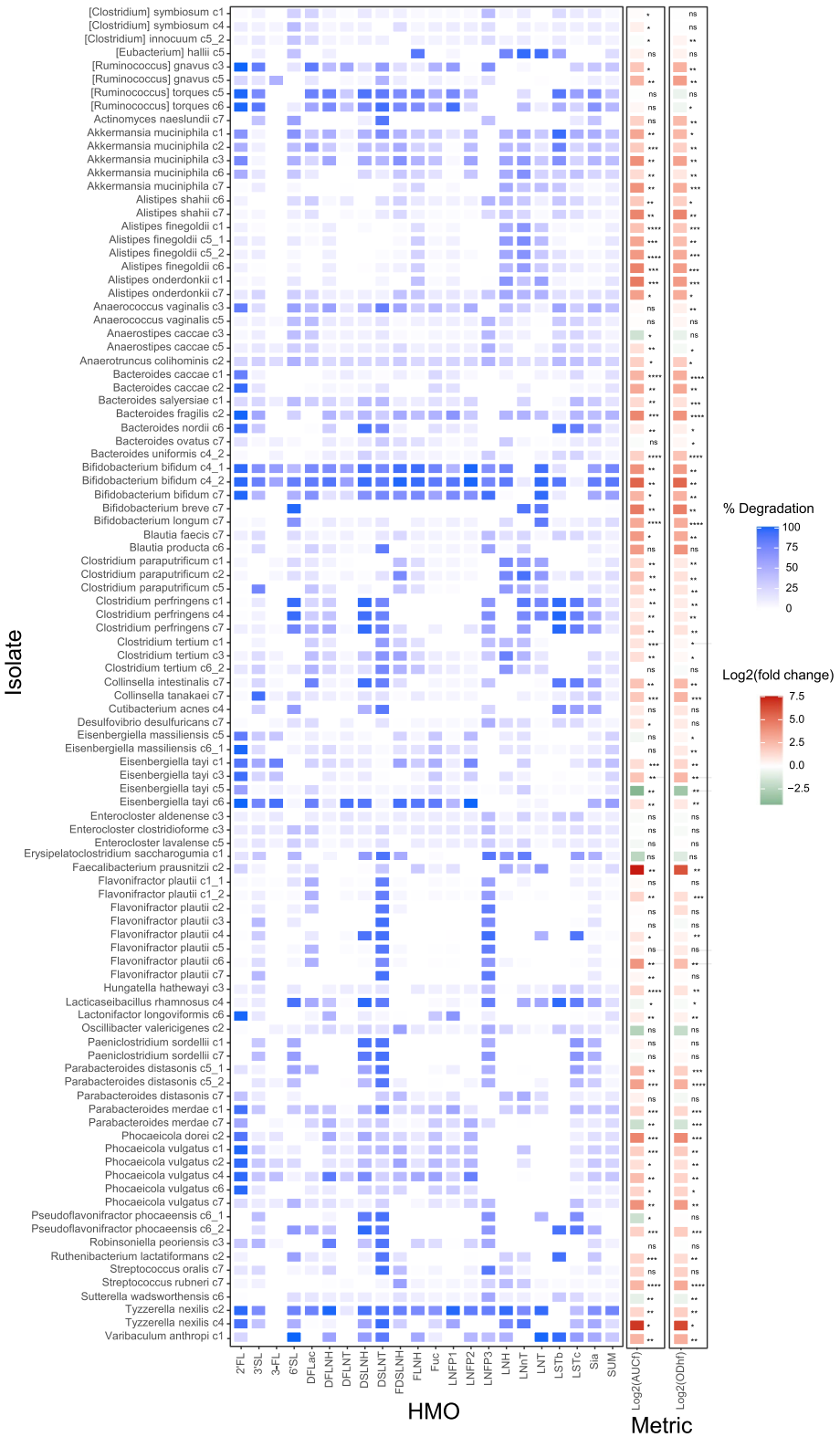

Fig. 5 Percent (%) degraded HMO structures and fold change in growth curve metrics of top 100 HMO-degrading bacterial isolates tested. Growth curve metrics are expressed as log2(AUCs in the presence of HMOs/AUCs in the control) (Log2(AUCf)) and log2(ODh in the presence of HMOs/ODh in the control) (Log2(ODhf)). Beside each fold change metric is the statistical significance of the difference between the treatment and control condition as determined using multiple *t*-tests with *p*-values corrected using the Benjamini-Hochberg method. ns non-significant; *$q < 0.05$;**$q < 0.01$; ***$q < 0.001$; ****$q < 0.0001$

Strain-dependent heterogeneity in HMO metabolism

As multiple isolates of several species were evaluated in this study, we next considered the intraspecies variation present in the ability to utilize HMOs among species with three or more isolates. In total, 181 isolates, belonging to 43 species, were separately clustered based on either growth curve metrics (Fig. 6A) or HMO structure degradation profiles (Fig. 6B). Isolates of the same species that consistently clustered together were determined to be homogeneous in their ability to utilize HMOs, while isolates of the same species that did not cluster together indicated cases of heterogeneity. Overall, intraspecies variation was observed for 35 species in at least one clustering assessment (Fig. 6C). Interestingly, variation in growth responses did not always correspond with different HMO degradation profiles. For example, intraspecies variation was observed in isolates of *Bacteroides* spp. where some isolates thrived in the presence of pHMOs while others were inhibited despite consistency in their HMO degradation profiles. In contrast, minimal differences were observed in the growth curves produced by isolates of some species, e.g., *Clostridium tertium*, but variation arose in their HMO structure specificities. Additionally, while the majority of the *Clos. innocuum* and *Phocaeicola vulgatus* isolates tested showed prolific HMO degradation, one isolate of each species exhibited only minimal degradation of the detectable HMO structures despite displaying enhanced growth following treatment. Lastly, all eight isolates of *Flav. plautii* avidly degraded LNFP3 and DSLNT, but only one isolate substantially utilized LSTc and DSLNH as well.

Discussion

Although infant formula supplemented with individual HMOs was found to be associated with health benefits for infants enrolled in clinical trials [9–12], there is a dearth of information on the ability of HMOs administered outside of human milk to alter the gut microbiota of young children. As such, we sought to compare the ability of 0.5 g/L 2'FL, the HMO most widely added to infant formula, and 4.0 g/L pHMOs, which reflect the full spectrum of HMOs present in human milk, to modulate microbial communities derived from healthy young post-weaned children. Given that the pHMOs mixture contained 0.5 g/L 2'FL, this concentration was used for direct comparisons between the impact of 2'FL alone and the same amount of 2'FL delivered alongside other HMOs naturally found in human milk. This design allowed us to assess the unique and combined effects of 2'FL within the broader context of HMO diversity.

Transitioning to a solid food diet correlates with a shift in the glycoside hydrolase profile of the child gut microbiota to support the metabolism of plant-derived oligosaccharides [22]. Despite this transition, the microbial communities in the current study retained the capacity to hydrolyze the most common HMO structures, suggesting that HMO-utilizing genes persist in the gut microbiota beyond weaning. Among the communities, Child_3 exhibited a limited ability to degrade certain larger HMO structures reflecting that a lower taxonomic diversity and associated reduced repertoire of functional processes may impede access to the benefits of some HMO structures. These findings underscore that supplementation with a broad range of HMO structures may be essential to maximize access to the benefits provided by these complex structures, which may be crucial for supporting gut microbiotas with limited taxonomic diversity.

Incubation with pHMOs unsurprisingly resulted in dramatic shifts in both community composition and metabolic activity that would likely be considered beneficial in a host environment such as an increased abundance of butyrate-producing taxa, e.g., *Roseburia* and *Faecalibacterium* [23]. Interestingly, *Bifidobacterium* was not the most proliferative taxa upon exposure to pHMOs, conceivably due to a potential reduction in *B. infantis* abundance as a result of weaning. Instead, members of the genus *Bacteroides* appeared to benefit the most from treatment with pHMOs, though their proliferation does not necessarily indicate primary degradation (direct metabolism) of HMOs. These increases may also result from secondary degradation (metabolism of the by-products from primary degradation), which warrants further investigation through axenic culture and characterization to elucidate the mechanisms by which isolates optimize HMOs.

Despite the heterogeneity in taxonomic composition across the microbial communities, their metabolic responses to pHMOs were largely similar. These included elevated production of the SCFA, acetate, and other organic acids, such as lactate and succinate, which together are the main fermentation products of indigestible oligosaccharides [24]. These metabolites are vital to host health, serving as nutrient sources and signaling molecules that influence host cell gene expression. SCFAs, for example, are known to stimulate intestinal epithelial cells and immune cells to promote production of anti-inflammatory cytokines and differentiation of naïve T cells into regulatory T cells [25]. Additionally, pHMOs stimulated the de novo biosynthesis of various amino acids, enhancing their availability for protein assembly and other bioactive molecules. Evidence from in vivo studies has shown that microbially derived amino acids can enter the host's plasma and become incorporated into host proteins [26]. pHMOs also lowered the production of disease-associated metabolites, such as

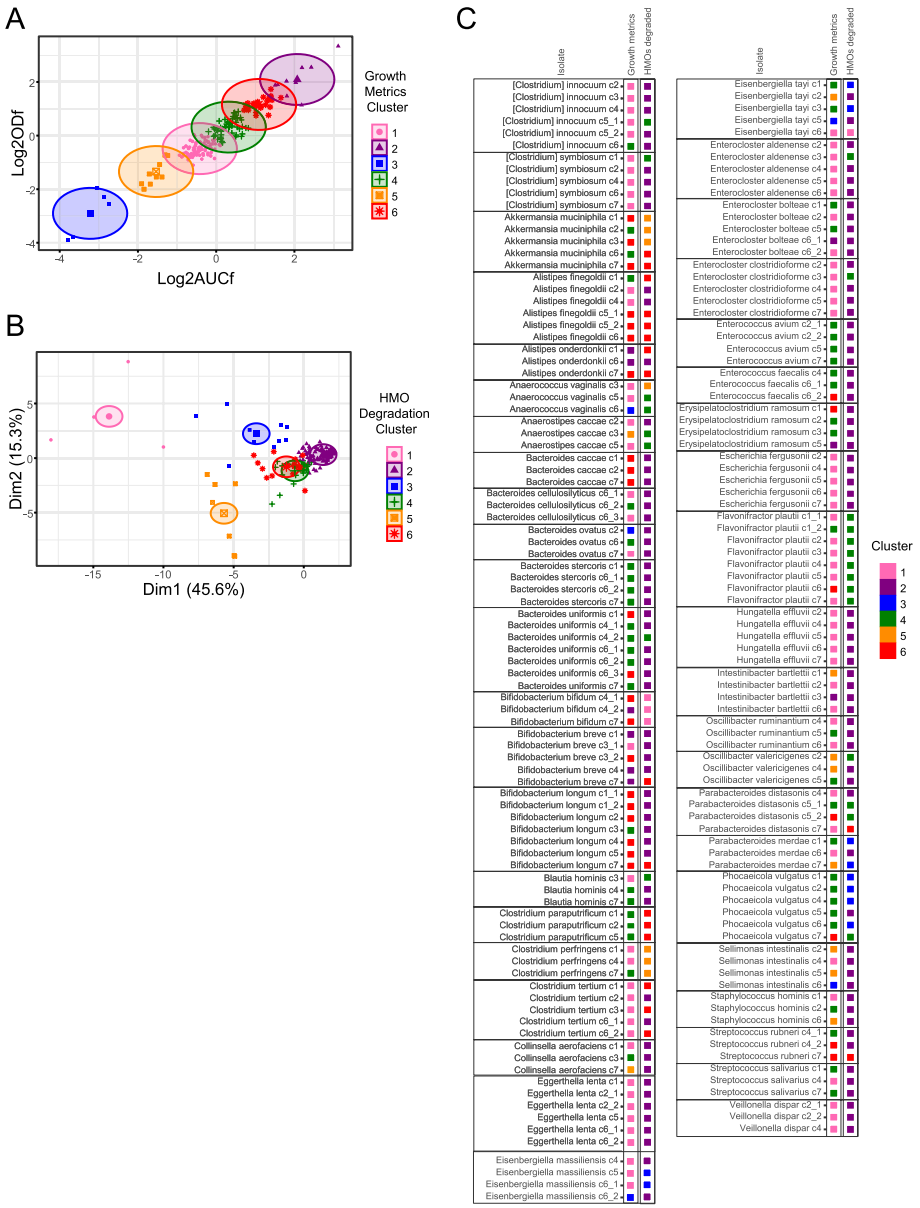

Fig. 6 Strain-dependent heterogeneity in HMO utilization abilities among species with three or more isolates treated with the pHMOs mixture as determined by k-means clustering based on their **A** growth metrics (log2(AUCs in the presence of HMOs/AUCs in the control) (Log2(AUCf)) and log2(ODh in the presence of HMOs/ODh in the control) (Log2(ODhf))) or **B** HMO degradation profiles. **C** Clusters into which all isolates assessed for heterogeneity were categorized based on Fig. 6A, B. Isolates of the same species that consistently clustered together were considered homogeneous in their ability to utilize HMOs, whereas isolates of the same species that clustered separately indicated heterogeneity

p-cresol, a phenolic compound found to inhibit cell respiration and proliferation and decrease gut barrier function in in vitro cultures of colonocytes [27, 28]. Overall, these shifts in the microbial communities induced by pHMOs treatment highlight their potential to enhance the health of young children by positively modulating their gut microbiota.

Prior research investigating the influence of 2'FL on microbial communities cultured in bioreactors reported significant changes in composition. However, these studies primarily focused on the expansion of *Bifidobacterium* populations, while other community members experienced only modest shifts in abundance [29–32]. In our study, 2'FL alone did not induce any significant changes in community composition or activity including within the *Bifidobacterium* genus. This suggests that only a subset of post-weaned infants may harbor *Bifidobacterium* strains capable of fermenting 2'FL. Notably, only the

Child_3 community exhibited a discernible metabolic change following 2'FL treatment, suggesting that the ability to metabolize and derive benefits from 2'FL is further subject to individual variability.

While the mechanisms employed by *Bifidobacterium* species to metabolize HMOs are being actively researched, less abundant members of the gut microbiota have been understudied despite their contribution to health. Here, we tested 330 bacterial isolates cultured from the aforementioned microbial communities to assess their ability to metabolize HMOs. We observed that a far wider diversity of species interacts with HMOs than was previously recognized, including members of 101 non-*Bifidobacterium* species that proliferated in the presence of HMOs. Recent studies have shown that HMOs can suppress the growth of pathogenic *Streptococcus agalactiae* (Group B Streptococcus (GBS)) and *Acinetobacter baumannii*, possibly by increasing membrane permeability to antibiotics [2, 33, 34]. However, since antibiotics were not included in the assay medium, we hypothesize that a novel antimicrobial mechanism driven by HMOs may be at play against certain isolates, which would require further study. Additionally, some isolates proliferated in the presence of HMOs despite little to no degradation of the quantified HMO structures, likely due to non-catabolic interactions as previously observed by Hunt et al. [35].

Congruent with past studies that tested multiple isolates of the same species for HMO utilization [5], we observed a high degree of intraspecies variation with more than half the species tested displaying strain-level heterogeneity. The 'pan-genome' of a species refers to the complete collection of genes present across its strains. Previous pan-genome analysis of gut-derived bacteria revealed that Bacteroidota members tend to have relatively expansive and open pan-genomes, while Bacillota members exhibit less variability, and Actinomycetota members display more constrained pan-genomes [36]. Nevertheless, studies of the *Bif. longum* pan-genome still demonstrated substantial genetic diversity at the strain level for carbohydrate metabolic capabilities including for the utilization of 2'FL and 3FL [37]. Therefore, it is evident that strain-level heterogeneity in HMO metabolism represents a common feature among constituents of the young child gut microbiota.

Overall, our study demonstrates the capacity of the gut microbiota of post-weaned young children to metabolize HMOs and derive benefits from their metabolism. However, several limitations should be considered when interpreting our findings. While exploring the effects of HMOs on fecal communities from young children provides valuable insights into their potential to modulate the post-weaned gut microbiota, particularly in contexts where prolonged breastfeeding or HMO supplementation may help prevent conditions like type 1 diabetes, it is important to note that the gut microbiota of these children may not be as optimized for HMO utilization as that of younger, breastfed infants. As such, stool samples from younger infants who are still breastfeeding may yield different results that reflect a microbiota more adapted to HMO metabolism. In addition, while we selected 4.0 g/L pHMOs and 0.5 g/L 2'FL to compare the effects of 2'FL alone versus it's equivalent amount within an HMO mixture, this approach does not account for the potential impact of providing equivalent total carbohydrate amounts between the treatments. Furthermore, our experimental setup lacked other infant formula components that reach the distal colon, such as galacto-oligosaccharides, fructo-oligosaccharides, lactoferrin, and partially hydrolyzed proteins. These components may influence the gut microbiota composition and function and may contribute to the broader modulatory effects of infant formula. Consequently, the results observed from the 2'FL supplementation in this study do not directly translate to the overall effects of infant formulae containing 2'FL. Lastly, several modern infant formulae now incorporate multiple HMO structures, with some formulations including up to five structures [11]. These may elicit broader microbiota-modulating effects than the single 2'FL treatment tested in this study. Future research could investigate various blends of HMOs and implement more frequent sampling in isolate assays to identify shifts in HMO preferences as favored HMOs are depleted, thereby shedding light on adaptive microbial strategies. This could be complemented by whole-genome sequencing to link genetic potential to these metabolic shifts, along with transcriptomics and proteomics to identify enzymatic pathways activated during HMO utilization. Such approaches would enable a deeper exploration of microbial adaptation and the mechanisms of HMO utilization, providing valuable insights into microbiota modulation within the context of infant diets.

Conclusion

This study has advanced our understanding of the health-enhancing properties of HMOs while highlighting the need for further studies on the efficacy of incorporating individual structures into infant formula, particularly when aiming to modulate the gut microbiota. By comprehensively characterizing HMO utilization in the largest collection of gut bacteria to date, we have demonstrated that HMOs interact with a wide diversity of non-*Bifidobacterium* species inclusive of those recognized for the potential health benefits as well as potential pathogens. Furthermore, our findings at both the community and

species levels underscore the considerable inter-individual variability in the capacity to derive health benefits from exogenously administered HMOs, a characteristic that necessitates thoughtful consideration when contemplating the use of HMOs for therapeutic applications, such as their inclusion in infant formula. It is imperative to recognize that HMO supplementation is not a one-size-fits-all paradigm where a single or few structures can adequately support gut microbiotas of all types.

Supplementary Information

The online version contains supplementary material available at https://doi.org/10.1186/s40168-025-02034-9.

Supplementary Material 1: Table S1. Characteristics of the 7 young children enrolled in the DIABIMMUNE birth cohort who donated the stool samples used in this study. Table S2. Concentration and percent (%) relative abundance of 19 common individual HMOs in the pooled HMOs (pHMOs) mixture. Table S3. Media types used to isolate bacteria from chemostat culture. Table S4. Reagents in modified peptone-yeast-glucose (mPYG) broth. Table S5. MaAsLin2 comparison of the effect of 4.0 g/L pHMOs, 0.5 g/L 2′FL, or no treatment on the absolute abundance of the genera in the microbial communities. Table S6. Tukey's honestly significant difference (HSD) pair-wise comparisons of auto-scaled metabolite concentrations 60 h after treatment of the microbial communities with 4.0 g/L pHMOs, 0.5 g/L 2′FL, or no treatment. Table S7. Bacterial strains isolated from fecal-derived microbial communities in bioreactors. Table S8. Statistical comparison of growth curve metrics.

Supplementary Material 2: Figure S1. Weighted UniFrac at each time point following treatment of the microbial communities with 4.0 g/L pHMOs, 0.5 g/L 2′FL or no treatment coloured by (A) microbial community or (B) treatment. Significance was determined using ADONIS (PERMANOVA) analyses.

Supplementary Material 3: Figure S2. Concentration of metabolites produced by the microbial communities following treatment with 4.0 g/L pHMOs, 0.5 g/L 2′FL, or no treatment.

Supplementary Material 4: Figure S3. Growth curves of 330 fecal-derived bacterial isolates, spanning 157 species, in the presence of 15 g/L pHMOs.

Supplementary Material 5: Figure S4. Percent (%) HMO degradation profiles of 330 fecal-derived bacterial isolates, spanning 157 species, 48 h after treatment with 15 g/L pHMOs categorized by phylum. (A) Actinomycetota; (B) Lentisphearota; (C) Pseudomonadota; (D) Verrucomicrobia; (E) Bacteroidota; (F) Bacillota.

Supplementary Material 6: Figure S5. Correlations among HMOs degraded by bacterial isolates and fold change in growth curve metrics as determined using Spearman's rank correlation coefficient.

Acknowledgements
We thank the AAC Genomics Facility and NMR Centre at the University of Guelph. We thank the DIABIMMUNE Consortium of researchers, clinicians, technologists, and families who made this study possible.

Authors' contributions
E.A.-V, L.B., and J.D. designed the research. S.R. and A.F. performed experiments. S.R. analyzed and interpreted experiments. S.R. performed bioinformatic analysis. M.K. and the DIABIMMUNE study group provided participants' samples and clinical metadata. S.R. wrote the manuscript, which all authors reviewed and edited.

Funding
This work was funded by operating grants from the Canadian Institutes of Health Research (CIHR), the JDRF (J.D. and E.A.-V.), the Anne and Max Tanenbaum Chair in Molecular Medicine, University of Toronto (J.D.), the Hospital for Sick Children Research Institute (J.D.) and the Canada Research Chairs Program (E, A,-V). L.B. is the UC San Diego Chair of Collaborative Human Milk Research endowed in perpetuity by the Family Larsson-Rosenquist Foundation, Switzerland. The DIABIMMUNE study was supported by a grant from the European Union Seventh Framework Program (grant number 202063) and a grant from the Academy of Finland (Centre of Excellence in Molecular Systems Immunology and Physiology; grant number 250114).

Data availability
All unique resources generated in this study may be available from the lead contact under a material transfer agreement. The 16S rRNA gene sequencing dataset is available in the NCBI database with BioProject ID PRJNA1094576 and SRA accession SAMN40701351 to SAMN40701728 (https://www.ncbi.nlm.nih.gov/bioproject/PRJNA1094576/). The metabonomics dataset was deposited on the MetaboLights [38] public repository and are available under the dataset accession number MTBLS9853 (www.ebi.ac.uk/metabolights/MTBLS9853). The R scripts for performing the bioinformatics analyses in this study are hosted at https://github.com/SimoneRenwick/Microbiome2024 (accessed on 23rd May 2024).

Declarations

Ethics approval and consent to participate
Selected fecal samples from the DIABIMMUNE sample database were shipped to the Allen-Vercoe lab following secondary site approval for culture and analysis by the University of Guelph Research Ethics Board, project REB#17-06-006.

Consent for publication
Not applicable.

Competing interests
E.A.-V. is a co-founder of Nubiyota, a company focused on the human gut microbiome. L.B. is a co-inventor on patent applications related to the use of HMOs in preventing NEC and other inflammatory diseases. S.R., A.F., M.K. and J.D. declare that they have no competing interests.

Received: 30 May 2024 Accepted: 8 January 2025
Published online: 07 February 2025

References

1. Bode L. Human milk oligosaccharides: every baby needs a sugar mama. Glycobiology. 2012;22:1147–62.
2. Ackerman DL, Doster RS, Weitkamp JH, Aronoff DM, Gaddy JA, Townsend SD. Human milk oligosaccharides exhibit antimicrobial and antibiofilm properties against Group B Streptococcus. ACS Infect Dis. 2017;3:595–605.
3. Kong C, Elderman M, Cheng L, de Haan BJ, Nauta A, de Vos P. Modulation of intestinal epithelial glycocalyx development by human milk oligosaccharides and non-digestible carbohydrates. Mol Nutr Food Res. 2019;63:1900303.
4. Castillo-Courtade L, Han S, Lee S, Mian FM, Buck R, Forsythe P. Attenuation of food allergy symptoms following treatment with human milk oligosaccharides in a mouse model. Allergy. 2015;70:1091–102.
5. Salli K, Hirvonen J, Siitonen J, Ahonen I, Anglenius H, Maukonen J. Selective utilization of the human milk oligosaccharides 2′-fucosyllactose, 3-fucosyllactose, and difucosyllactose by various probiotic and pathogenic bacteria. J Agric Food Chem. 2021;69:170–82.
6. Bode L. The functional biology of human milk oligosaccharides. Early Hum Dev. 2015;91:619–22.
7. Kunz C, Meyer C, Collado MC, Geiger L, García-Mantrana I, Bertua-Ríos B, et al. Influence of gestational age, secretor, and lewis blood group status on the oligosaccharide content of human milk. J Pediatr Gastroenterol Nutr. 2017;64:789–98.
8. Zhu Y, Luo G, Wan L, Meng J, Lee SY, Mu W. Physiological effects, biosynthesis, and derivatization of key human milk tetrasaccharides, lacto-N-tetraose, and lacto-N-neotetraose. Crit Rev Biotechnol. 2021;42:1–19.
9. Marriage BJ, Buck RH, Goehring KC, Oliver JS, Williams JA. Infants fed a lower calorie formula with 2′FL show growth and 2′FL uptake like breast-fed infants. J Pediatr Gastroenterol Nutr. 2015;61:649–58.

10. Puccio G, Alliet P, Cajozzo C, Janssens E, Corsello G, Sprenger N, et al. Effects of infant formula with human milk oligosaccharides on growth and morbidity: a randomized multicenter trial. J Pediatr Gastroenterol Nutr. 2017;64:624–31.
11. Parschat K, Melsaether C, Jäpelt KR, Jennewein S. Clinical evaluation of 16-week supplementation with 5HMO-Mix in healthy-term human infants to determine tolerability, safety, and effect on growth. Nutrients. 2021;13: 2871.
12. Goehring KC, Marriage BJ, Oliver JS, Wilder JA, Barrett EG, Buck RH. Similar to those who are breastfed, infants fed a formula containing 2′-fucosyllactose have lower inflammatory cytokines in a randomized controlled trial. J Nutr. 2016;146:2559–66.
13. Berger PK, Plows JF, Jones RB, Alderete TL, Yonemitsu C, Poulsen M, et al. Human milk oligosaccharide 2′-fucosyllactose links feedings at 1 month to cognitive development at 24 months in infants of normal and overweight mothers. PLoS One. 2020;15:1–12.
14. Vatanen T, Jabbar KS, Ruohtula T, Honkanen J, Avila-Pacheco J, Siljander H, et al. Mobile genetic elements from the maternal microbiome shape infant gut microbial assembly and metabolism. Cell. 2022;185:4921–36.
15. Gianetto-Hill CM, Vancuren SJ, Daisley B, Renwick S, Wilde J, Schroeter K, et al. The Robogut: a bioreactor model of the human colon for evaluation of gut microbial community ecology and function. Curr Protoc. 2023;3:e737.
16. Jantscher-Krenn E, Zherebtsov M, Nissan C, Goth K, Guner YS, Naidu N, et al. The human milk oligosaccharide disialyllacto-N-tetraose prevents necrotising enterocolitis in neonatal rats. Gut. 2012;61:1417–25.
17. Oliphant K, Parreira VR, Cochrane K, Allen-Vercoe E. Drivers of human gut microbial community assembly: coadaptation, determinism and stochasticity. ISME J. 2019;13:3080–92.
18. Callahan BJ, McMurdie PJ, Rosen MJ, Han AW, Johnson AJA, Holmes SP. DADA2: High-resolution sample inference from Illumina amplicon data. Nat Methods. 2016;13:581–3.
19. Ganobis CM, Al-Abdul-Wahid MS, Renwick S, Yen S, Carriero C, Aucoin MG, et al. 1D 1H NMR as a tool for fecal metabolomics. Curr Protoc Chem Biol. 2020;12:e83.
20. Berger PK, Hampson HE, Schmidt KA, Alderete TL, Furst A, Yonemitsu C, et al. Stability of human-milk oligosaccharide concentrations over 1 week of lactation and over 6 hours following a standard meal. J Nutr. 2022;152:2727–33.
21. Mallick H, Rahnavard A, McIver LJ, Ma S, Zhang Y, Nguyen LH, et al. Multivariable association discovery in population-scale meta-omics studies. PLoS Comput Biol. 2021;17: e1009442.
22. Ioannou A, Knol J, Belzer C. Microbial glycoside hydrolases in the first year of life: an analysis review on their presence and importance in infant gut. Front Microbiol. 2021;12:12.
23. Lordan C, Thapa D, Ross RP, Cotter PD. Potential for enriching next-generation health-promoting gut bacteria through prebiotics and other dietary components. Gut Microbes. 2020;11:1–20.
24. Oliphant K, Allen-Vercoe E. Macronutrient metabolism by the human gut microbiome: major fermentation by-products and their impact on host health. Microbiome. 2019;7:1–15.
25. Lee W-J, Hase K. Gut microbiota–generated metabolites in animal health and disease. Nat Chem Biol. 2014;10:416–24.
26. Neis EPJG, Dejong CHC, Rensen SS. The role of microbial amino acid metabolism in host metabolism. Nutrients. 2015;7:2930–46.
27. McCall IC, Betanzos A, Weber DA, Nava P, Miller GW, Parkos CA. Effects of phenol on barrier function of a human intestinal epithelial cell line correlate with altered tight junction protein localization. Toxicol Appl Pharmacol. 2009;241:61–70.
28. Andriamihaja M, Lan A, Beaumont M, Audebert M, Wong X, Yamada K, et al. The deleterious metabolic and genotoxic effects of the bacterial metabolite p-cresol on colonic epithelial cells. Free Radic Biol Med. 2015;85:219–27.
29. Van den Abbeele P, Duysburgh C, Vazquez E, Chow J, Buck R, Marzorati M. 2′-Fucosyllactose alters the composition and activity of gut microbiota from formula-fed infants receiving complementary feeding in a validated intestinal model. J Funct Foods. 2019;61:103484.
30. Nogacka AM, Arboleya S, Nikpoor N, Auger J, Salazar N, Cuesta I, et al. Influence of 2′-fucosyllactose on the microbiota composition and metabolic activity of fecal cultures from breastfed and formula-fed infants at two months of age. Microorganisms. 2021;9: 1478.
31. Van den Abbeele P, Sprenger N, Ghyselinck J, Marsaux B, Marzorati M, Rochat F. A comparison of the *in vitro* effects of 2′fucosyllactose and lactose on the composition and activity of gut microbiota from infants and toddlers. Nutrients. 2021;13:726.
32. Li H, Lane JA, Chen J, Lu Z, Wang H, Dhital S, et al. *In vitro* fermentation of human milk oligosaccharides by individual *Bifidobacterium longum*-dominant infant fecal inocula. Carbohydr Polym. 2022;287:119322.
33. Ackerman DL, Craft KM, Doster RS, Weitkamp J-H, Aronoff DM, Gaddy JA, et al. Antimicrobial and antibiofilm activity of human milk oligosaccharides against *Streptococcus agalactiae*, *Staphylococcus aureus*, and *Acinetobacter baumannii*. ACS Infect Dis. 2017;4:315–24.
34. Lin AE, Autran CA, Szyszka A, Escajadillo T, Huang M, Godula K, et al. Human milk oligosaccharides inhibit growth of group B Streptococcus. J Biol Chem. 2017;292:11243–9.
35. Hunt KM, Preuss J, Nissan C, Davlin CA, Williams JE, Shafii B, et al. Human milk oligosaccharides promote the growth of staphylococci. Appl Environ Microbiol. 2012;78:4763–70.
36. Zou Y, Xue W, Luo G, Deng Z, Qin P, Guo R, et al. 1,520 reference genomes from cultivated human gut bacteria enable functional microbiome analyses. Nat Biotechnol. 2019;37:179–85.
37. Arboleya S, Bottacini F, O'Connell-Motherway M, Ryan CA, Ross RP, Van Sinderen D, et al. Gene-trait matching across the *Bifidobacterium longum* pan-genome reveals considerable diversity in carbohydrate catabolism among human infant strains. BMC Genomics. 2018;19:1–16.
38. Yurekten O, Payne T, Tejera N, Amaladoss FX, Martin C, Williams M, et al. MetaboLights: open data repository for metabolomics. Nucleic Acids Res. 2024;52:D640–6.

Publisher's Note